I&EC research
Industrial & Engineering Chemistry Research
pubs.acs.org/IECR
Article

On the Reduction of Power Consumption in Vortexing Unbaffled Bioslurry Reactors

Francesca Scargiali, Alberto Brucato, Giorgio Micale, and Alessandro Tamburini*

Cite This: *Ind. Eng. Chem. Res.* 2020, 59, 8037−8045
Read Online
ACCESS | Metrics & More | Article Recommendations

ABSTRACT: Bioremediation of polluted soils via bioslurry reactors is an interesting option among those available nowadays, especially when recalcitrant pollutants are present. Vortexing unbaffled stirred tanks may be a valuable choice to this purpose as they were recently found to be more efficient than baffled vessels for solid suspension processes where mixing time is not a controlling factor. When operated at sufficiently high agitation speeds, the central vortex bottom reaches the impeller and air bubbles start to be distributed throughout the system, thus avoiding any sparger and related clogging issues. In the present work, a vortexing unbaffled stirred tank with solid loadings ranging from 2.5% w/w (weight of the solid/weight of the liquid) up to the very high 160% w/w was studied. Different turbine types including Rushton turbine, up- and down-pumping pitched blade turbines, and A310 were investigated. The minimum impeller speeds for complete particles' suspension (N_{js}) and system aeration (N_{cr}) along with the relevant power (P_{js}, P_{cr}) and specific power (per mass unit) consumptions (ε_{js}, ε_{cr}) were assessed, in order to identify the geometrical configuration and operating condition providing the lowest power consumption. Results showed that the Rushton turbine and a solid concentration B of about 30% may be the most economically convenient arrangement to achieve system aeration and complete particles' suspension at the same time inside the reactor.

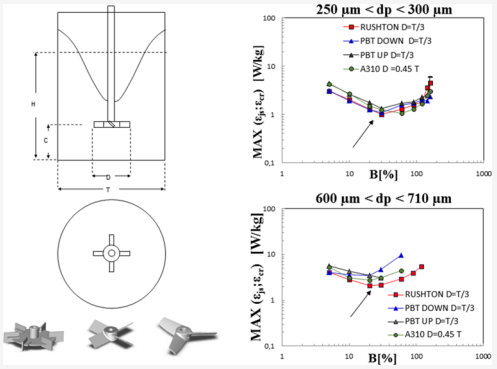

1. INTRODUCTION

Soils' pollution of industrial sites is a crucial problem of the last decades. Therefore, the attention to novel and effective remediation technologies is continuously increasing.

In situ bioremediation is generally easier to be carried out but, in the case of low permeability or particularly heterogeneous soils, it is not always effective.[1] As an alternative, *ex situ* bioremediation processes resulted in efficient removal of pesticides, polycyclic aromatic hydrocarbons (PAHs), petroleum hydrocarbons, solvents, and so forth from polluted soils.[2−4]

Unfortunately, conventional bioremediation processes may require dramatically high treatment times, especially when resistant waste products such as PAHs are present.[5]

Biological reactors operating in a slurry phase might be an effective technology to decrease recalcitrant pollutants' concentration in feasible times.[6,7] In these bioreactors, contaminated soil is mixed with water, nutrients, air, and other additives. The reactor is commonly equipped with process control systems devoted to creating ideal conditions for the biodegradation, thus guaranteeing an effective degradation pace, even when resistant contaminants are present.[8] More importantly, such systems are provided with stirrers that mechanically agitate the slurry in order to increase mass transfer coefficients and the related bioremediation rates.[9]

This is why a number of studies have been recently devoted to the bioremediation of polluted soils via bioslurry reactor technology,[10−14] although operational costs are still high.[15] In order to make the process more efficient, optimization of the tank hydrodynamic performance may play an important role and boost the technology development. Moreover, high solid particle concentration is requested during reactor loading in order to maximize the mass of solid per reactor unit volume[16,17] and proper aeration systems should be used in order to avoid possible sparger hole clogging.[18] To this purpose, vortexing unbaffled stirred tanks may be a more suitable choice, compared to traditional sparged gas−liquid stirred vessels. In vortexing unbaffled tanks, at low rotational speeds ($N < N_{cr}$, *i.e., subcritical conditions*), the free surface vortex does not reach the impeller and gas−liquid mass transfer occurs through the vortex free surface,[19] leading to volumetric mass transfer coefficients being adequate for some

Received: February 12, 2020
Revised: March 27, 2020
Accepted: April 1, 2020
Published: April 1, 2020

https://dx.doi.org/10.1021/acs.iecr.0c00726
Ind. Eng. Chem. Res. 2020, 59, 8037−8045

biological processes.[20] At larger rotational speeds, the central vortex reaches the impeller ($N = N_{cr}$, *i.e. critical conditions*) and, at slightly larger N ($N \geq N_{cr}$, *i.e., supercritical conditions*), air begins to be ingested and dispersed inside the reactor in the form of tiny bubbles, thus promoting gas−liquid mass transfer.[21] In this way, a k_La comparable to those obtained in sparged stirred tanks[22,23] can be reached without the aforementioned sparger holes clogging issues typical of traditional bioslurry gas−liquid reactors.[24,25] Additionally, at $N = N_{cr}$ the homogenization efficiency of unbaffled vessels was found equal to that of more common baffled stirred tanks.[26]

In bioslurry reactors, solid particles' suspension is fundamental for a successful bioremediation of contaminated soils[27,28] and the well-known just-suspension rotational speed N_{js} is largely considered the right compromise choice to achieve a satisfying solid−liquid interfacial area with reasonable stirring costs.[29−31] Unbaffled stirred reactors have been found to be particularly effective for particle suspension, requiring lower power consumptions per unit volume, than standard baffled tanks.[32,33]

Many studies have dealt with complete particles' suspension[34,35] or system aeration,[20−22] whereas no attempts have been devoted yet to investigating the two aspects at the same time.

In this work, experiments were carried out in a vortexing unbaffled stirred vessel with solid loadings ranging from 2.5% w/w (weight of the solid/weight of the liquid) up to the very high 160% w/w. Different turbine types, including Rushton turbine (RT), up- and down-pumping pitched blade turbines (PBTs), and Lightnin A310 were investigated. N_{js} and N_{cr} along with their relevant specific power requirements ε_{js} and ε_{cr} were assessed in order to identify the best impeller geometry and the "optimal" solid loading guaranteeing at the same time solid suspension and liquid aeration with minimum specific power requirements.

2. EXPERIMENTAL SECTION

The experimental apparatus was a cylindrical unbaffled stirred vessel with T = 0.19 m diameter (Figure 1). The vessel was filled with water up to a height $H = T$. Two kinds of monodispersed soil particles (silica) purposely sieved were employed (d_p = 250−300 μm and d_p = 600−710 μm and density $\rho \approx 2400$ kg/m^3). Monodispersed soils were prudentially investigated in order to exclude any effect of particles' dispersion during the results analysis.

The diameter ranges (*i.e.,* 250−300 and 600−710 μm) derive from the mesh size of the sieves employed to sieve them. These two sizes were chosen because they have been extensively investigated in the literature[36−38] to observe particles' size effect.[39−41] High solid loadings per unit volume are typically used in bioremediation reactors in order to maximize the reactor efficiency. For this reason, in this work, the investigated solid particles' concentrations ranged from 2.5% w/w (weight of the solid/weight of the liquid) up to the very high 160% w/w, corresponding to a volumetric concentration ranging from 1 to 40% v/v (volume of solids/total reactor volume). Three different turbine geometries were investigated (Figure 2): RT with $D = T/3$, PBT with $D = T/3$, and Lightnin A310 with $D = 0.45T$.

Lightnin A310 with $D = T/3$ was also initially tested but, as it did not allow complete suspension conditions to be achieved for $B > 5\%$, it was excluded from the results. Impeller clearance C was set at one-third of the tank diameter ($C = T/3$) in all the

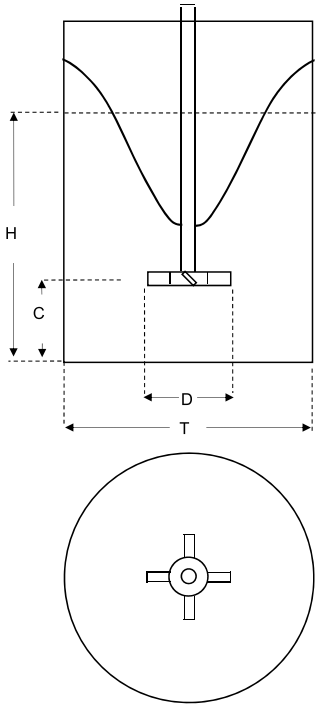

Figure 1. Sketch of the experimental apparatus.

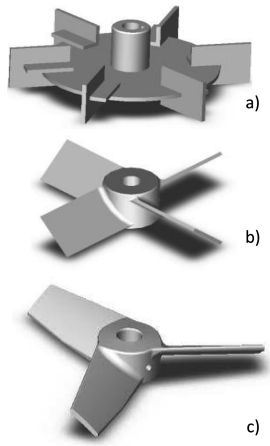

Figure 2. Turbines investigated: (a) RT; (b) PBT; (c) Lightnin A310 turbine.

investigated cases. Regarding oxygen supply necessary to microorganisms[42] in real systems, no gas distributor was used and oxygen mass transfer occurred through the free surface vortex for $N < N_{cr}$ and through the ingested air bubbles' surface when the agitation speed is sufficient for air-entrapping ($N > N_{cr}$).

2.1. N_{js} Measurements. The minimum impeller speed ensuring the suspension of all particles (N_{js}) was assessed by means of the well-known "*one second criterion*".[43] According to this criterion, particles are considered fully suspended (*complete suspension*) if none of them stays motionless on the vessel bottom for more than one second. To reduce visual subjectivity, a video camera placed underneath the vessel bottom was employed.[44] The shutter opening time was set to one second as prescribed by Zwietering's criterion. In this way, motionless particles had neat contours in the images, whereas all moving particles were blurred. N_{js} was defined as the first

https://dx.doi.org/10.1021/acs.iecr.0c00726
Ind. Eng. Chem. Res. 2020, 59, 8037−8045

agitation speed at which no particles had neat contours in the recorded images. Twenty different images per each agitation speed were recorded and analyzed. It is worth noting that this method allows the identification of the just suspension speed in accordance with the "on-bottom" definition: according to this definition, particles rolling on the vessel bottom are considered as suspended. On-bottom suspension is considered sufficient to guarantee an adequate renewal of the liquid phase surrounding the particles, thus allowing solid−liquid mass transfer to occur efficiently.

2.2. N_{cr} Measurements. N_{cr} is the minimum agitation speed at which the air vortex reaches the impeller blades and the gas phase begins to be ingested and dispersed in the liquid as tiny bubbles, while the system is becoming three-phasic (*complete aeration*).

In the gas−liquid−solid system, visual inspection is difficult because of the presence of particles, which make the system opaque. In order to assess the rotational speed at which vortex free surface reaches the impeller plane (N_{cr}) and gas bubbles begin to be ingested inside the liquid phase, a simple criterion named "*hearing criterion*"[45] was employed. It is based on the distinct noise produced by the rotating turbine when it is ingesting air: N_{cr} was identified as the minimum speed at which this noise was heard. Visual inspection revealed that it corresponded to the first velocity at which the turbine is not fully covered by the liquid phase. Different operators repeated each test three times, and a very good reproducibility was found: maximum discrepancy was about 5%.

2.3. Power Input Measurements. The power drawn by each turbine was measured, thanks to a homemade system composed of a static frictionless turntable placed on a precision scale. The apparatus consists of a granite support holding the tank, rotating around its axis, and a system including a laboratory scale, a wire, and a pulley that allowed measuring the force necessary to prevent vessel rotation. Details on this inexpensive homemade apparatus can be found in Scargiali et al.[19]

In order to compare the present unbaffled tank with the more common baffled systems, suitable measurements were taken in a corresponding tank provided with baffles (whose width was $b = T/10$).

3. RESULTS AND DISCUSSION

3.1. Minimum Impeller Speed for Just Complete Suspension and Aeration. The minimum rotational speed necessary to achieve just suspension conditions (N_{js}) is reported in Figure 3 as a function of solids' loading (B %) for small (Figure 3a) and large particles (Figure 3b), respectively.

As it can be seen, N_{js} increases as B % increases in both figures, but a different dependence can be observed at B % higher than ~30% ($N_{js} \propto B^{0.13}$ for B % < 30% and $N_{js} \propto B^{0.54}$ for B > 30%). A possible interpretation of this result may be that for particle concentrations larger than a certain value, system rheology changes because of particle interactions and a higher dependence of N_{js} on B % is observed. This behavior is found both for small and large particles. In addition, the N_{js} values obtained do not change very much with particles' size as already observed in other works.[32] For comparison purposes, the N_{js} values calculated by means of the Zwietering correlation for the case of RT with $D = T/3$ (the configuration providing the lowest N_{js} in the baffled systems) are reported in the same figure. As shown in the figure, for particle

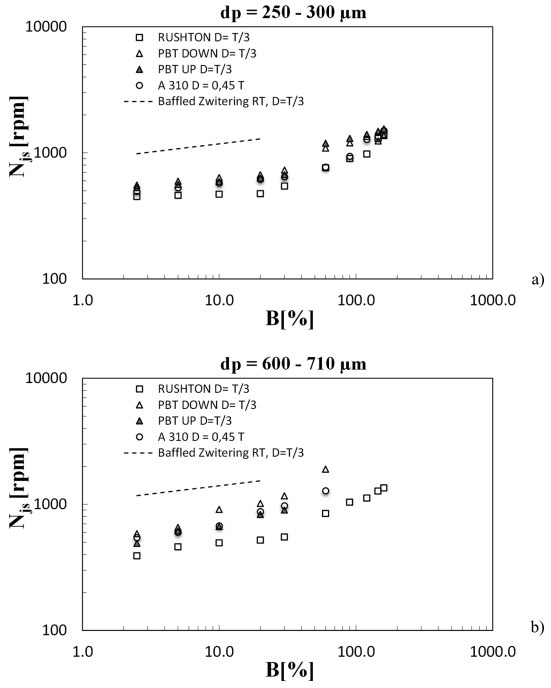

Figure 3. Minimum rotational speed necessary to achieve just suspension conditions *vs* solids loading for different impeller geometries: (a) small particles; (b) large particles. The dashed line represents N_{js} in baffled systems calculated via Zwietering's correlation.

concentrations B % lower than 20%, the just suspended velocities relevant to the baffled configuration are much larger than those experimentally obtained in the unbaffled vessel, whereas a comparison is not possible for B % larger than 20% as Zwietering's correlation is not reliable at large solid loadings.[46−48] The lowest N_{js} values are obtained with the RT. Notably, for the case of large particles and some turbines (*i.e.,* PBT and A310) complete suspension conditions were not achieved, even at very large N. This is not surprising because when the vortex reaches the turbine blades and the system is aerated, the fluid-dynamics conditions completely change, and the turbine suspension capability may dramatically reduce. Such a behavior was already observed by Nagata[49] who tried to identify the aeration conditions under which suspension is not possible (for given particles and turbines).

Regarding system aeration, critical rotational speed (N_{cr}) for the investigated turbines is shown in Figure 4a,b as a function of B % for small and large particles, respectively. At solids' concentrations lower than about 60%, the achievement of aeration conditions is weakly influenced by solids' loading, whereas a steep increase of N_{cr} is observed when the solids' concentration becomes larger (*i.e.,* $N_{cr} \approx$ const. for B < 60% and $N_{cr} \propto B^{0.95}$ for B > 60%). This may be the consequence of a certain effect of solid particles' concentration increase on the vortex features: the high solid loadings lead the solid−liquid two-phase system to behave like a one-phase slurry system, thus completely modifying the fluid dynamics of the system including the interaction with the gas-phase.

Clearly, at this stage only hypotheses can be made, as additional data are needed to fully understand the phenomenon: to this purpose, local data provided by computational fluid dynamics simulations might be a viable solution.

https://dx.doi.org/10.1021/acs.iecr.0c00726
Ind. Eng. Chem. Res. 2020, 59, 8037−8045

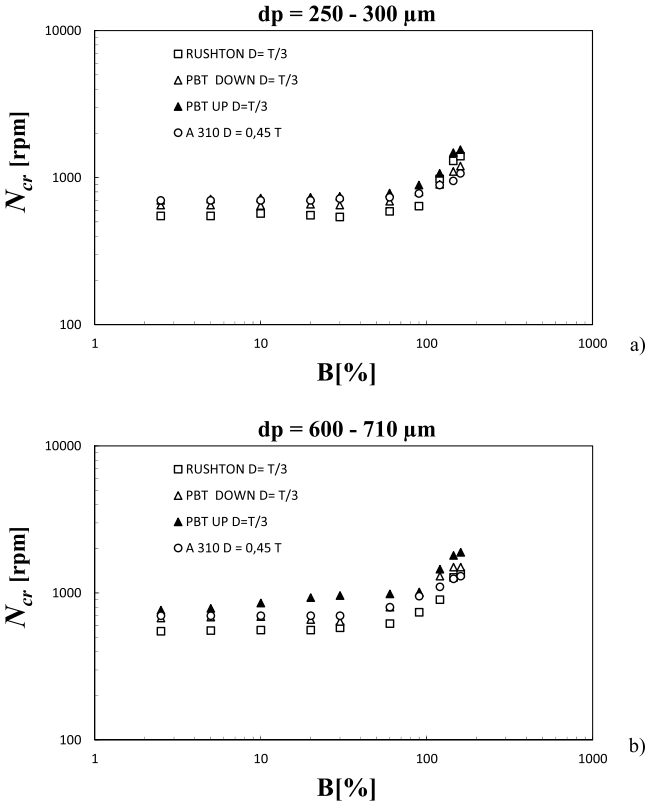

Figure 4. Critical rotational speed necessary to achieve complete aeration conditions (N_{cr}) *vs* solids' loading for different impeller geometries: (a) small particles; (b) large particles.

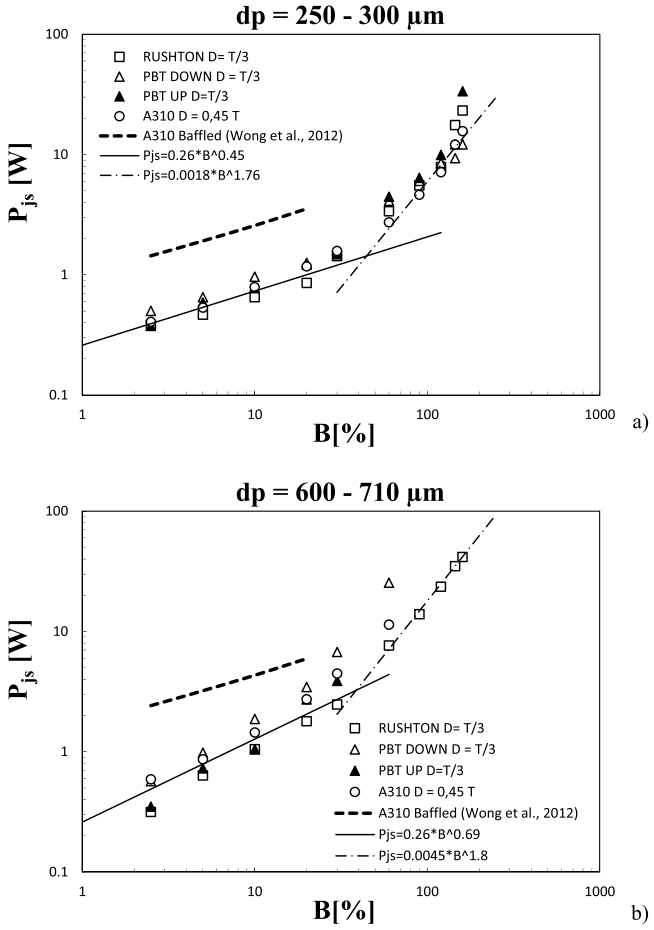

Figure 5. Power consumption necessary to just suspend particles (P_{js}) *vs* solids' loading for different impeller geometries: (a) small particles; (b) large particles.

Notably, also in the aeration case, the lowest N_{cr} values are obtained with the RT.

3.2. Minimum Power Consumption for Just Complete Suspension and Aeration. N_{js} and N_{cr} represent a valuable piece of information, although corresponding power requirements are more suitable to perform a comparison among different geometrical configurations. Therefore, in Figure 5a,b, the minimum power requirement needed to just suspend all particles, P_{js} (*i.e,.* power measured at $N = N_{js}$), was reported as a function of solids' loading for small and large particles, respectively. The values experimentally assessed are compared with those relevant to a baffled tank stirred by an A310 stirrer that represents the most efficient configuration observed in baffled tanks.[44] In this case (*i.e.,* baffled tanks) the P_{js} was estimated from the power number expression, $N_p = P_{js}/(\rho_{susp} N_{js}^3 D^5)$, where N_p was set to 0.36 from experimental measurements performed at B % = 0, and N_{js} was calculated using Zwietering's correlation with a geometrical value S inferred from Wong et al.[50] data.

As shown in Figure 5a,b, the P_{js} values measured in the vortexing unbaffled configuration are much lower than the corresponding ones referring to the best option available for baffled tanks (*i.e.,* A310 turbine), advising the unbaffled system as economically convenient. On the other hand, a similar dependence of P_{js} on B % was found for the two configurations, especially for the lower particle size. The comparison is limited to B % lower than 20%, as unreliable predictions may be provided by Zwietering's correlation at larger B %.[51] Interestingly, it can be observed that the lowest P_{js} values are mostly obtained with the RT.

The lower power requirements of the unbaffled configuration with respect to the baffled one may be due to the diverse particle suspension mechanism leading to different N_{js} values. In unbaffled tanks, among the possible suspension mechanisms, the *avoidance of settling*[52] may be the prominent one, because of the high centrifugal force and the lack of obstacles (baffles). This is not the case in baffled tanks, where velocities on the vessel bottom are allegedly lower and the *off-bottom lifting*[52] is expected to be the controlling suspension phenomenon. Clearly, the lack of baffles likely leads to the lower power consumptions in the unbaffled tanks. Besides particle suspension, the different particle distribution in the two tanks may also play an important role. At a given N_{js}, in baffled tanks, local concentrations are higher in the stirrer region,[53,54] whereas in radially stirred unbaffled tanks, solid particles' distribution is preferentially concentrated far from the stirrer,[55−57] thanks to the higher centrifugal forces. Thus, the different distribution probably adds another effect linked to the different apparent density seen by the impeller. It is worth noting that the reduction of N_{js} in unbaffled vessels should not be considered as the result of the different N_{js} definition (*off-bottom* in Zwietering's correlation and *on-bottom* in the present work). This is confirmed by the fact that other authors observed the same reduction in completely different conditions. For instance, Tezura et al.[36] investigated an unbaffled vessel stirred by an unsteadily forward-reverse rotating impeller and compared the measured N_{js} with

https://dx.doi.org/10.1021/acs.iecr.0c00726
Ind. Eng. Chem. Res. 2020, 59, 8037−8045

Zwietering's correlation (valid for baffled vessels unidirectionally stirred). Notwithstanding, in the two cases the suspension mechanism is expected to be the same (*i.e., off-bottom lifting*), the N_{js} values measured in their unbaffled system were lower than the ones pertaining to the corresponding baffled system. Wang et al.[37] compared unbaffled and baffled tanks (unidirectionally) stirred and assessed N_{js} by employing the particle bed height method[58] (instead of the Zwietering one), which does not discriminate between *on-bottom* and *off-bottom* suspension and found again lower N_{js} in the unbaffled system.

Concerning the P_{js} *vs* B % trend, as already observed for N_{js}, the relation between P_{js} and B % is a power law with two different exponents, depending on the solids' loading. At low solid loadings (B < 20%), P_{js} results proportional to $B^{0.45}$ for d_p = 250−300 μm, whereas P_{js} results proportional to $B^{0.69}$ for d_p = 600−710 μm. At larger particles' concentrations (B > 20%), a slight increase in the value of B % results in a much larger power consumption increase. Apart from few points (those at the largest B %), this higher dependence can be roughly represented by a power law (*i.e.,* $P_{js} \propto B^{\sim 1.8}$ both for small and large particles).

A similar behavior can be observed for the critical power consumption P_{cr} necessary to aerate the system. As it can be seen in Figure 6a,b, for B %<60%, P_{cr} exhibits a low dependence on B % (*i.e.,* $P_{cr} \propto B^{0.24}$ for small particles and $P_{cr} \propto B^{0.32}$ for large particles), whereas for larger particle concentrations achieving aeration conditions becomes more power-demanding ($P_{cr} \propto B^{1.8}$ for small particles and $P_{cr} \propto B^{1.9}$ for large particles). Concerning the turbine comparison, the down pumping PBT was found the most efficient for the lowest solid concentrations, andthe A310 turbine for the larger concentrations.

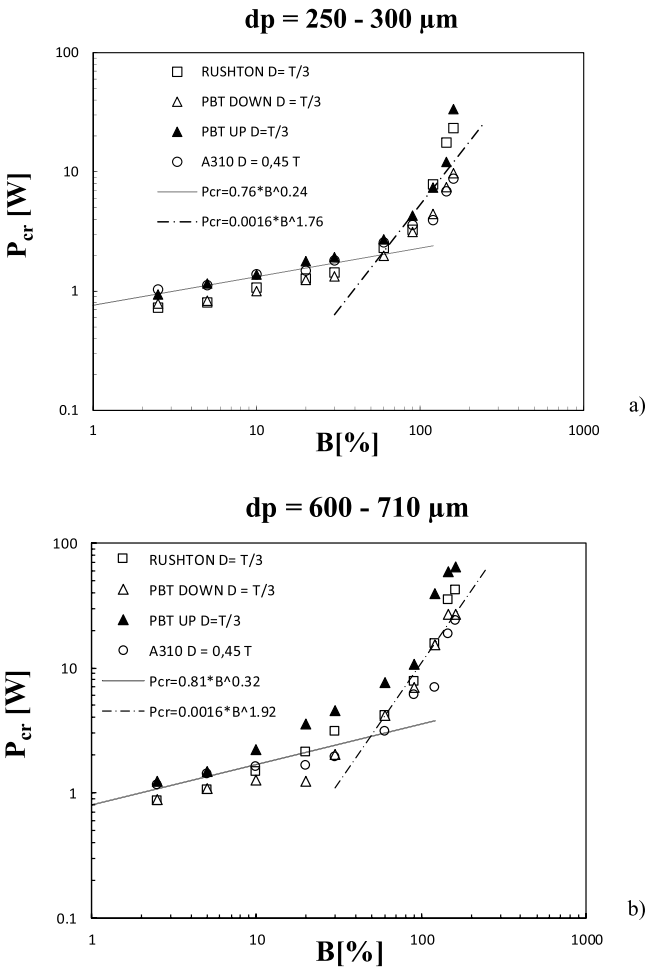

Figure 6. Power consumption necessary to achieve aeration conditions (P_{cr}) *vs* solids' loading for different impeller geometries: (a) small particles; (b) large particles.

Notably, as a difference from critical rotational speed N_{cr}, the critical power consumption P_{cr} shows some dependence on B % also at low solid loadings. This is because when particle concentration is increasing but it is still low (*i.e., B* in the range 0−30%), the vortex depth reaches the turbine disk at a very similar N, whereas the concentration of the solution swept by the turbine is increasing with B %. Thus, the increase of P_{cr} with B % within the range 0−30% may be due to apparent density effects.

3.3. Specific Power Consumption for Just Complete Suspension and Aeration. In bioslurry reactors, it is important to minimize the remediation cost for the unit mass of contaminated soil.[16] This is why power consumption per unit mass of solids, easily assessed as the ratio between power requirements and particles' loading, is a parameter of paramount importance. As two different phenomena (*i.e.,* solid suspension and system aeration) are investigated in this work, two different specific power parameters were consequently defined: the specific power consumption for particle suspension (ε_{js}) and the specific power consumption for system aeration (ε_{cr}). The analysis of these two quantities is expected to allow the identification of the geometrical configurations (*viz* impeller types) and operating conditions (*viz* solids loading), guaranteeing the highest cost savings.

In Figure 7a,b, the dependence of ε_{js} on B % is reported for small and large particles respectively. In Figure 7a, ε_{js} exhibits a decreasing−increasing dependence on B %, so resulting in relative minima whose exact position depends on the impeller type: this falls between 20 and 30% in most cases. Moreover, it can be observed that, as far as particle suspension is concerned, the simple RT along with a solid/liquid concentration ≈ B % = 20% results in the lowest power demand amongst the configurations here investigated. It is worth noting that operating the tank under different conditions may result in a quite dramatic increase of the specific power consumption. Just as an example, operating at B = 2.5% results in more than tripling the specific power consumption and significantly reducing the process economic performance. This latter result was also reported by Wang et al.[33] for the case of a nonaerated solid−liquid unbaffled system.

Regarding the larger particles here investigated, Figure 7b shows that the required specific power consumptions are larger with respect to the smaller particles, as expected. Similarly to the previous case, the curves show specific minima. More important, the standard RT is once again the best impeller type, whereas the optimal particle loading is about 30%. It can also be observed, however, that a 20% loading would not result in large changes of suspension efficiency. The range 20−30% for B % may be regarded as an "*optimal solids' loading for just suspension*" at which the tank should be operated to minimize operation costs for complete suspension.

Similar considerations apply to the case of the critical specific power consumption to aerate the system, ε_{cr}. As reported in Figure 8a,b, also the ε_{cr} *vs* B % trend is nonmonotonic and exhibits minima that roughly occur between B % = 60 and 80% for small particles, and between

https://dx.doi.org/10.1021/acs.iecr.0c00726
Ind. Eng. Chem. Res. 2020, 59, 8037−8045

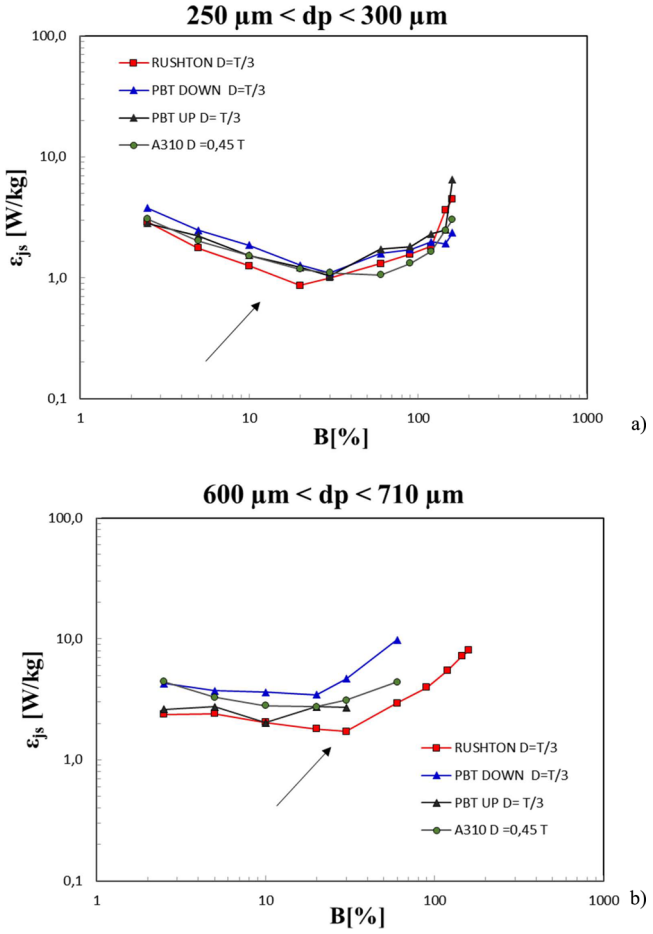

Figure 7. Specific power consumption necessary to suspend 1 kg of solids (P_{js}/M_s) *vs* solids' loading for different impeller geometries: (a) small particles; (b) large particles. Arrows indicate the most efficient solids/liquid % to achieve just suspension.

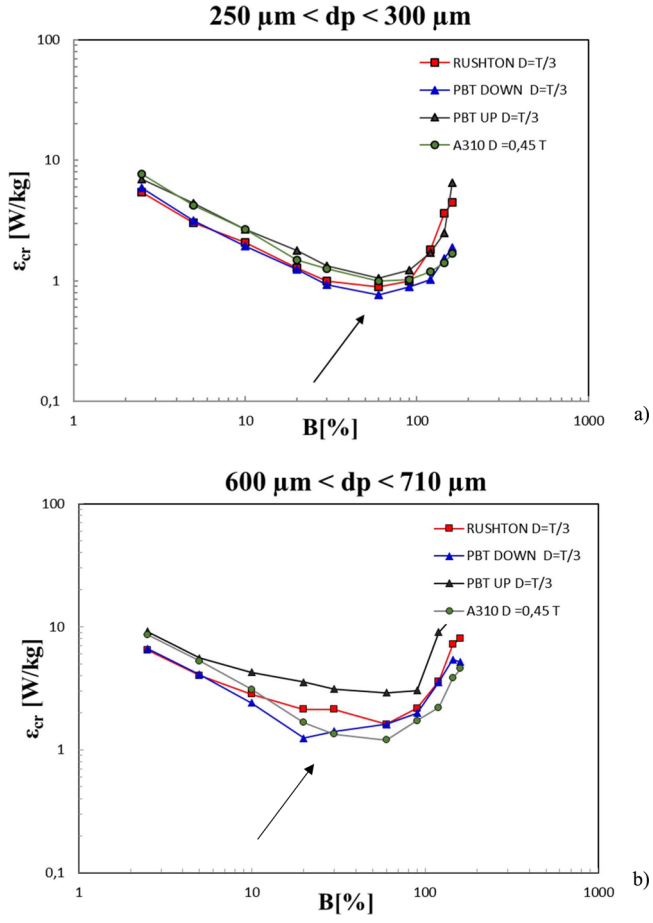

Figure 8. Specific power consumption necessary to aerate 1 kg of solids (P_{cr}/M_s) *vs* solids' loading for different impeller geometries: (a) small particles; (b) large particles. Arrows indicate the most efficient solids/liquid % to aerate the system.

20 and 60% for large particles. These values of B %, may be regarded as the "*optimal solids' loading for complete aeration*", which should be adopted to minimize operation costs when system aeration is the mostly desired process condition. In case only system aeration is required, the down pumping PBT impeller with a solid/liquid concentration B = 60% will be the best choice for smaller particles (250 μm < d_p < 300 μm); conversely, for larger particles (600 μm < d_p < 710 μm), A310 with a solid/liquid concentration B = 60% would be the most convenient choice.

3.4. Identification of the Best Operating Condition. The choice of the best operating condition will depend on the specific process, taking into account whether it is more important either particle suspension or gas dispersion. For instance, different processes (e.g., including different bacteria and substrates) may not require a particularly large oxygen demand. In these cases, oxygen mass transfer through the free surface vortex may be sufficient to sustain the process without any need of gas dispersion[59,60] and, therefore, the above discussion on ε_{js} should drive the choice of the optimal operating conditions.

Conversely, in case both aeration and suspension are needed, the best combination between impeller geometry and particles' concentration must be selected by referring to both processes. In order to evaluate which is the most efficient impeller geometry to both suspend particles and aerate the system, it is useful to plot the maximum value between ε_{js} and ε_{cr}, max(ε_{js};ε_{cr}), against the relevant solid concentration B %. This is done in Figure 9a,b for the four turbine geometries here tested.

In Figure 9a, for small particles (250−300 μm), the most efficient combination between impeller geometry and solid/liquid concentration can be obtained by the RT at a solid/liquid concentration B % = 30%. It may be worth noting that also the down pumping PBT and Lightnin A310 at solid/liquid concentrations B % = 30 and 60%, respectively, lead to similar optimal conditions. Regarding large particles (600−710 μm), the most efficient combination is represented by the RT at a solid/liquid concentration $B \approx$ 20−30%.

Considerations like those relevant to Figures 7−9 can be inferred also from Figure 10a,b where ε_{js} is plotted against ε_{cr} for the four turbine geometries analyzed and the various solid particles' concentrations. In these figures, each curve refers to one turbine geometry, whereas each point of the curves is relevant to one of the solid/liquid concentrations investigated.

For systems where only particle suspension is needed, data points closer to the vertical axis represent the more efficient configuration. When system aeration is the most important phenomenon, data points closer to the horizontal axis guarantee lower power consumptions. If both complete suspension and aeration are equally important, the best combination between impeller geometry and solid/liquid

https://dx.doi.org/10.1021/acs.iecr.0c00726
Ind. Eng. Chem. Res. 2020, 59, 8037−8045

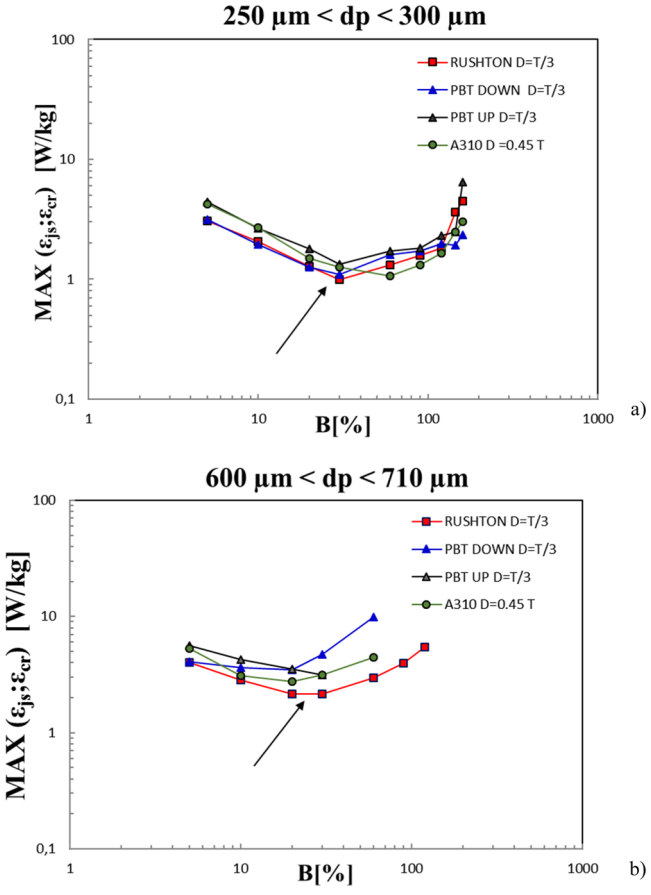

Figure 9. Specific power consumption necessary to contemporaneously suspend and aerate 1 kg of solids ($\max[P_{js};P_{cr}]/M_s$) *vs* solids' loading for different impeller geometries: (a) small particles; (b) large particles. Arrows indicate the most efficient solids/liquid % to both suspend and aerate the system.

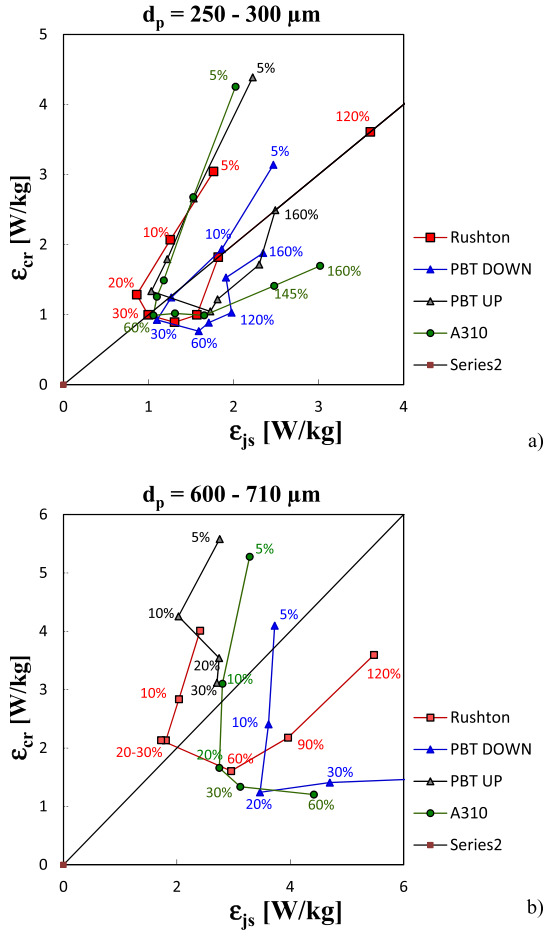

Figure 10. Specific power consumptions at the critical rotational speed (ε_{cr}) *vs* specific power consumption at the just suspension speed (ε_{js}) at various solid/liquid concentrations (B %): (a) particle diameter d_p = 250−300 μm; (b) particle diameter d_p = 600−710 μm. red square = RT; blue triangle = PBT down pumping; gray triangle = PBT up-pumping; green circle = Lightnin A310 turbine.

concentration will be given by the points of the curves nearest the origin of the axes (both ε_{js} and ε_{cr} very low).

In addition, Figure 10 also indicates that, for low particle concentrations, aerating the system is more power-demanding than just suspending particles, whereas, at high solid loadings, complete suspension costs more than system aeration.

4. CONCLUSIONS

In the present work, a vortexing *unbaffled* stirred tank was investigated in view of its use as a bioslurry reactor.

Summarizing, depending on bioreaction rates, two process categories may be identified:

(a) processes not requiring system complete aeration and where therefore only particle suspension is important. For such processes, the present results show that the optimal combination of impeller type and particles' concentration is given by the RT with a solid loading of about 20% for smaller particles (250−300 μm) and 30% for larger particles (600−710 μm).

(b) processes requiring system complete aeration in addition to particle suspension. For these processes, the specific power dissipation adopted must be equal to or larger than the maximum between ε_{js} and ε_{cr}. For these systems, the collected results indicate that, for smaller particles (250−300 μm), the RT at a solid/liquid concentration B % = 30% is the optimal combination between impeller type and particles concentration. However, the down-pumping PBT or the Lightnin A310 at a solid/liquid concentrations B % = 30 and 60% respectively may be a valid alternative. Regarding large particles (600−710 μm), the most efficient combination is given by the RT at a solid/liquid concentration B % = 20−30%.

Overall, the adoption of a standard RT and particles' concentration of the order of 30% appears to be a sensible choice for most bioslurry processes, independently of particle size and oxygen transfer rate requirements.

AUTHOR INFORMATION

Corresponding Author

Alessandro Tamburini − *Dipartimento di Ingegneria, Università di Palermo, 90128 Palermo, Italy;* orcid.org/0000-0002-0183-5873; Phone: +39 09123863780; Email: alessandro.tamburini@unipa.it

Authors

Francesca Scargiali − *Dipartimento di Ingegneria, Università di Palermo, 90128 Palermo, Italy;* orcid.org/0000-0003-4049-9806

https://dx.doi.org/10.1021/acs.iecr.0c00726
Ind. Eng. Chem. Res. 2020, 59, 8037−8045

Alberto Brucato − *Dipartimento di Ingegneria, Università di Palermo, 90128 Palermo, Italy*
Giorgio Micale − *Dipartimento di Ingegneria, Università di Palermo, 90128 Palermo, Italy*

Complete contact information is available at: https://pubs.acs.org/10.1021/acs.iecr.0c00726

Notes

The authors declare no competing financial interest.

NOMENCLATURE

B	particle concentration as solid-weight/liquid-weight (%)
C	vessel clearance [m]
D	impeller diameter [m]
d_p	particle diameter [m]
g	acceleration gravity, [m s^{-2}]
H	liquid height [m]
k_L	mass transfer coefficient [m s^{-1}]
k_La	volumetric mass transfer coefficient [s^{-1}]
M_s	mass of solids [kg]
N	rotational speed [s^{-1}]
N_{cr}	critical rotational speed for system aeration [s^{-1}]
N_{js}	rotational speed for particles just suspension [s^{-1}]
N_p	power number [—]
P	power input [W]
P_{cr}	power consumption at N_{cr} [W]
P_{js}	power consumption at N_{js} [W]
PBT	pitched blade turbine
RT	Rushton turbine
T	tank diameter [m]
ε_{cr}	specific power consumption for system aeration [W kg^{-1}]
ε_{js}	specific power consumption for particles' just suspension [W kg^{-1}]
μ,	liquid viscosity [Pa·s]
ρ_L	liquid density [kg m^{-3}]
ρ_{susp}	solid−liquid suspension density [kg m^{-3}]

REFERENCES

(1) Sanscartier, D.; Reimer, K.; Zeeb, B.; Koch, I. The Effect of Temperature and Aeration Rate on Bioremediation of Diesel-Contaminated Soil in Solid-phase Bench-Scale Bioreactors. *Soil Sedim. Contam. Cont.* **2011**, *20*, 353−369.
(2) Sylva, T. Y.; Kinoshita, C. M.; Romano, R. T.; Toma, M.; Tsang, S. K.; Chang, K. Bioremediation of Petroleum-Impacted Soils from Investigation-Derived Wastes. *Remediation* **2003**, *13*, 79−90.
(3) Quintero, J. C.; Lú-Chau, T. A.; Moreira, M. T.; Feijoo, G.; Lema, J. M. Bioremediation of HCH present in soil by the white-rot fungus Bjerkandera adusta in a slurry batch bioreactor. *Int. Biodeterior. Biodegr.* **2007**, *60*, 319−326.
(4) Li, X.; Du, Y.; Wu, G.; Li, Z.; Li, H.; Sui, H. Solvent extraction for heavy crude oil removal from contaminated soils. *Chemosphere* **2012**, *88*, 245−249.
(5) Sanscartier, D.; Laing, T.; Reimer, K.; Zeeb, B. Bioremediation of weathered petroleum hydrocarbon soil contamination in the Canadian High Arctic: Laboratory and field studies. *Chemosphere* **2009**, *77*, 1121−1126.
(6) Lewis, R. F. SITE Demonstration of Slurry-Phase Biodegradation of PAH Contaminated Soil. *J. Air Waste Manag. Assoc.* **1993**, *43*, 503−508.
(7) Zappi, M. E.; Rogers, B. A.; Teeter, C. L.; Gunnison, D.; Bajpai, R. Bioslurry treatment of a soil contaminated with low concentrations of total petroleum hydrocarbons. *J. Hazard. Mater.* **1996**, *46*, 1−12.
(8) Tamburini, A.; Cipollina, A.; Micale, G.; Brucato, A. Measurements of Njs and power requirements in unbaffled bioslurry reactors. *Chem. Eng. Trans.* **2012**, *27*, 343−348.
(9) Cassidy, D.; Efendiev, S.; White, D. M. A comparison of CSTR and SBR bioslurry reactor performance. *Water Res.* **2000**, *34*, 4333−4342.
(10) Okieimen, C. O.; Okieimen, F. E. Effect of natural rubber processing sludge on the degradation of crude oil hydrocarbons in soil. *Bioresour. Technol.* **2002**, *82*, 95−97.
(11) Fuller, M.; Manning, J. F., Jr. Microbiological changes during bioremediation of explosives-contaminated soils in laboratory and pilot-scale bioslurry reactors. *Bioresour. Technol.* **2004**, *91*, 123−133.
(12) Shailaja, S.; Ramakrishna, M.; Venkata Mohan, S.; Sarma, P. N. Biodegradation of di-n-butyl phthalate (DnBP) in bioaugmented bioslurry phase reactor. *Bioresour. Technol.* **2007**, *98*, 1561−1566.
(13) Shailaja, S.; Venkata Mohan, S.; Rama Krishna, M.; Sarma, P. N. Degradation of di-ethylhexyl phthalate (DEHP) in bioslurry phase reactor and identification of metabolites by HPLC and MS. *Int. Biodeterior. Biodegr.* **2008**, *62*, 143−152.
(14) Ramakrishna, M.; Venkata Mohan, S.; Shailaja, S.; Narashima, R.; Sarma, P. N. Identification of metabolites during biodegradation of pendimethalin in bioslurry reactor. *J. Hazard. Mater.* **2008**, *151*, 658−661.
(15) Snellinx, Z.; Nepovím, A.; Taghavi, S.; Vangronsveld, J.; Vanek, T.; Van der Lelie, D. Biological remediation of explosives and related nitroaromatic compounds. *Environ. Sci. Pollut. Res.* **2002**, *9*, 48−61.
(16) Cassidy, D. P.; Irvine, R. L. The effect of operating conditions on theperformance of soil slurry-SBRs. *Water Sci. Technol.* **2001**, *43*, 223−230.
(17) Venkatamohan, S.; Ramakrishna, M.; Shailaja, S.; Sarma, P. Influence of soil-water ratio on the performance of slurry phase bioreactor treating herbicide contaminated soil. *Bioresour. Technol.* **2007**, *98*, 2584−2589.
(18) Busciglio, A.; Grisafi, F.; Scargiali, F.; Brucato, A. On the measurement of local gas hold-up and interfacial area in gas-liquid contactors via light sheet and image analysis. *Chem. Eng. Sci.* **2010**, *65*, 3699−3708.
(19) Scargiali, F.; Tamburini, A.; Caputo, G.; Micale, G. On the assessment of power consumption and critical impeller speed in vortexing unbaffled stirred tanks. *Chem. Eng. Res. Des.* **2017**, *123*, 99−110.
(20) Scargiali, F.; Busciglio, A.; Grisafi, F.; Brucato, A. Mass transfer and hydrodynamic characteristics of unbaffled stirred bio-reactors: influence of impeller design. *Biochem. Eng. J.* **2014**, *82*, 41−47.
(21) Scargiali, F.; Busciglio, A.; Grisafi, F.; Tamburini, A.; Micale, G.; Brucato, A. Power consumption in uncovered unbaffled stirred tanks: Influence of the viscosity and flow regime. *Ind. Eng. Chem. Res.* **2013**, *52*, 14998−15005.
(22) Labík, L.; Petričříček, R.; Moucha, T.; Brucato, A.; Caputo, G.; Grisafi, F.; Scargiali, F. Scale-up and viscosity effects on gas-liquid mass transfer rates in unbaffled stirred tanks. *Chem. Eng. Res. Des.* **2018**, *132*, 584−592.
(23) Petříček, R.; Labik, L.; Moucha, T.; Brucato, A.; Scargiali, F. Gas-liquid mass transfer rates in unbaffled tanks stirred by PBT: scale-up effects and pumping direction. *Chem. Eng. Res. Des.* **2018**, *137*, 265−272.
(24) Conway, K.; Kyle, A.; Rielly, C. D. Gas-Liquid-Solid Operation of a Vortex-Ingesting Stirred Tank Reactor. *Chem. Eng. Res. Des.* **2002**, *80*, 839−845.
(25) Scargiali, F.; Busciglio, A.; Grisafi, F.; Brucato, A. Gas-liquid-solid operation of a high aspect ratio self-ingesting reactor. *Int. J. Chem. React. Eng.* **2012**, *10*, A27.
(26) Busciglio, A.; Grisafi, F.; Scargiali, F.; Brucato, A. Mixing dynamics in uncovered unbaffled stirred tanks. *Chem. Eng. J.* **2014**, *254*, 210−219.
(27) Ibrahim, S.; Nienow, A. W. Suspension of microcarriers for cell culture with axial flow impellers. *Chem. Eng. Res. Des.* **2004**, *82*, 1082−1088.

(28) Ibrahim, S.; Jasnin, S. N.; Wong, S. D.; Baker, I. F. Zwietering's Equation for the Suspension of Porous Particles and the Use of Curved Blade Impellers. *Int. J. Chem. Eng.* **2012**, *2012*, 749760.
(29) Sardeshpande, M. V.; Sagi, A. R.; Juvekar, V. A.; Ranade, V. V. Solid Suspension and Liquid Phase Mixing in Solid−Liquid Stirred Tanks. *Ind. Eng. Chem. Res.* **2009**, *48*, 9713−9722.
(30) Ayranci, I.; Kresta, S. M. Critical analysis of Zwietering correlation for solids suspension in stirred tanks. *Chem. Eng. Res. Des.* **2014**, *92*, 413−422.
(31) Davoody, M.; Abdul Raman, A. A. B.; Parthasarathy, R. Maximizing Impeller Power Efficiency in Gas-Solid-Liquid Stirred Vessels through Process Intensification. *Ind. Eng. Chem. Res.* **2015**, *54*, 11915−11928.
(32) Brucato, A.; Cipollina, A.; Micale, G.; Scargiali, F.; Tamburini, A. Particle suspension in top-covered unbaffled tanks. *Chem. Eng. Sci.* **2010**, *65*, 3001−3008.
(33) Wang, S.; Parthasarathy, R.; Bong, E. Y.; Wu, J.; Slatter, P. Suspension of ultrahigh concentration solids in an agitated vessel. *AIChE J.* **2012**, *58*, 1291−1298.
(34) Wu, J.; Graham, L.; Nguyen, B. Mixing intensification for the mineral industry. *Can. J. Chem. Eng.* **2010**, *88*, 447−454.
(35) Wu, J.; Nguyen, B.; Lane, G.; Wang, S.; Parthasarathy, R.; Graham, L. J. Process Intensification in Stirred Tanks. *Chem. Eng. Technol.* **2012**, *35*, 1125−1132.
(36) Tezura, S.; Kimura, A.; Yoshida, M.; Yamagiwa, K.; Ohkawa, A. Agitation requirements for complete solid suspension in an unbaffled agitated vessel with an unsteadily forward-reverse rotating impeller. *J. Chem. Technol. Biotechnol.* **2007**, *82*, 672−680.
(37) Wang, S.; Boger, D. V.; Wu, J. Energy efficient solids suspension in an agitated vessel-water slurry. *Chem. Eng. Sci.* **2012**, *74*, 233−243.
(38) Wang, S.; Parthasarathy, R.; Wu, J.; Slatter, P. Optimum Solids Concentration in an Agitated Vessel. *Ind. Eng. Chem. Res.* **2014**, *53*, 3959−3973.
(39) Micheletti, M.; Nikiforaki, L.; Lee, K. C.; Yianneskis, M. Particle Concentration and Mixing Characteristics of Moderate-to-Dense Solid-Liquid Suspensions. *Ind. Eng. Chem. Res.* **2003**, *42*, 6236−6249.
(40) Van der Westhuizen, A. P.; Deglon, D. A. Solids suspension in a pilot-scale mechanical flotation cell: A critical impeller speed correlation. *Miner. Eng.* **2008**, *21*, 621−629.
(41) Tamburini, A.; Cipollina, A.; Micale, G.; Brucato, A.; Ciofalo, M. Influence of drag and turbulence modelling on CFD predictions of solid liquid suspensions in stirred vessels. *Chem. Eng. Res. Des.* **2014**, *92*, 1045−1063.
(42) Leunen, L. A.; Buggs, V. H.; Eestep, M. E.; Enriquez, R. C.; Leonerd, J. W.; Blaylock, M. J.; Huang, J. W.; Haggblom, M. M. Bioremediation of polyaromatic hydrocarbon contaminated sediments in aerated bioslurry reactors. *Bioremed. J.* **2002**, *6*, 125−141.
(43) Zwietering, T. N. Suspending of solid particles in liquid by agitators. *Chem. Eng. Sci.* **1958**, *8*, 244−253.
(44) Tamburini, A.; Brucato, A.; Busciglio, A.; Cipollina, A.; Grisafi, F.; Micale, G.; Scargiali, F.; Vella, G. Solid-Liquid Suspensions in Top-Covered Unbaffled Vessels: Influence of Particle Size, Liquid Viscosity, Impeller Size, and Clearance. *Ind. Eng. Chem. Res.* **2014a**, *53*, 9587−9599.
(45) Tamburini, A.; Cipollina, A.; Micale, G.; Scargiali, F.; Brucato, A. Particle Suspension in Vortexing Unbaffled Stirred Tanks. *Ind. Eng. Chem. Res.* **2016**, *55*, 7535−7547.
(46) Kasat, G. R.; Pandit, A. B. Review on mixing characteristics in solid-liquid and solid-liquid-gas reactor vessels. *Can. J. Chem. Eng.* **2008**, *83*, 618−643.
(47) Rieger, F.; Ditl, P. Suspension of solid particles in agitated vessels. In *Proceedings of the 4th European Conference on Mixing*; BHRA: Cranfield, U.K., 1982; p 263.
(48) Tamburini, A.; Cipollina, A.; Micale, G.; Brucato, A.; Ciofalo, M. CFD simulations of dense solid-liquid suspensions in baffled stirred tanks: Prediction of the minimum impeller speed for complete suspension. *Chem. Eng. J.* **2012b**, *193*−*194*, 234−255.
(49) Nagata, S. *Mixing − Principles and Applications*; Wiley: New York, 1975; pp 271−276.
(50) Wong, C. W.; Wang, J. P.; Huang, S. T. Investigations of fluid dynamics in mechanically stirred aerated slurry reactors. *Can. Jour. Chem. Eng.* **1987**, *65*, 412−419.
(51) Oldshue, J. Y., Sharma, R. N. *The Effect of Off-Bottom Distance of an Impeller for the 'Just Suspended Speed', Njs*; AIChE Symp. Ser.; American Institute of Chemical Engineers: New York, 1992; Vol. *88*, pp 72−78.
(52) Mersmann, A.; Werner, F.; Maurer, S.; Bartosch, K. Theoretical prediction of the minimum stirrer speed in mechanically agitated suspensions. *Chem. Eng. Proc.* **1998**, *37*, 503−510.
(53) Micheletti, M.; Nikiforaki, L.; Lee, K. C.; Yianneskis, M. Particle Concentration and Mixing Characteristics of Moderate-to-Dense Solid−Liquid Suspensions. *Ind. Eng. Chem. Res.* **2003**, *42*, 6236−6249.
(54) Carletti, C.; Montante, G.; Westerlund, T.; Paglianti, A. Analysis of solid concentration distribution in dense solid-liquid stirred tanks by electrical resistance tomography. *Chem. Eng. Sci.* **2014**, *119*, 53−64.
(55) Tamburini, A.; Gentile, L.; Cipollina, A.; Micale, G.; Brucato, A. Experimental investigation of dilute solid-liquid suspension in an unbaffled stirred vessel by a novel pulsed laser based image analysis technique. *Chem. Eng. Trans.* **2009**, *17*, 531−536.
(56) Tamburini, A.; Cipollina, A.; Micale, G.; Brucato, A. Particle distribution in dilute solid liquid unbaffled tanks via a novel laser sheet and image analysis based technique. *Chem. Eng. Sci.* **2013b**, *87*, 341−358.
(57) Wang, S.; Jiang, M.; Ibrahim, S.; Wu, J.; Feng, X.; Duan, X.; Yang, Z.; Yang, C.; Ohmura, N. Optimized Stirred Reactor for Enhanced Particle Dispersion. *Chem. Eng. Tech.* **2016**, *39*, 680−688.
(58) Hicks, M. T.; Myers, K. J.; Bakker, A. Cloud Height in Solids Suspension Agitation. *Chem Eng Comm* **1997**, *160*, 137−155.
(59) Chisti, Y. Animal-cell damage in sparged bioreactors. *Trends Biotechnol.* **2000**, *18*, 420−432.
(60) Scargiali, F.; Busciglio, A.; Grisafi, F.; Brucato, A. Free surface oxygen transfer in large aspect ratio unbaffled bio-reactors, with or without draft-tube. *Biochem. Eng. J.* **2015**, *100*, 16−22.

https://dx.doi.org/10.1021/acs.iecr.0c00726
Ind. Eng. Chem. Res. 2020, 59, 8037−8045